Atmos. Chem. Phys., 16, 2659–2673, 2016
www.atmos-chem-phys.net/16/2659/2016/
doi:10.5194/acp-16-2659-2016

Atmospheric Chemistry and Physics
Open Access
EGU

Oxygen isotope mass balance of atmospheric nitrate at Dome C, East Antarctica, during the OPALE campaign

Joël Savarino[1,2], William C. Vicars[1,2,a], Michel Legrand[1,2], Suzanne Preunkert[1,2], Bruno Jourdain[1,2], Markus M. Frey[3], Alexandre Kukui[4,5], Nicolas Caillon[1,2], and Jaime Gil Roca[4,5]

[1]Université Grenoble Alpes, Laboratoire de Glaciologie et Géophysique de l'Environnement (LGGE), 38000 Grenoble, France
[2]CNRS, Laboratoire de Glaciologie et Géophysique de l'Environnement (LGGE), 38000 Grenoble, France
[3]British Antarctic Survey, Natural Environment Research Council, Cambridge, UK
[4]Laboratoire Atmosphère, Milieux et Observations Spatiales (LATMOS), UMR8190, CNRS-Université de Versailles Saint Quentin, Université Pierre et Marie Curie, Paris, France
[5]Laboratoire de Physique et Chimie de l'Environnement et de l'Espace (LPC2E), UMR6115 CNRS-Université d'Orléans, 45071 Orléans CEDEX 2, France
[a]now at: Technical Services Program, Air Pollution Control Division, Colorado Department of Public Health and Environment, Denver, CO, USA

Correspondence to: Joël Savarino (jsavarino@ujf-grenoble.fr)

Received: 26 June 2015 – Published in Atmos. Chem. Phys. Discuss.: 7 September 201
Revised: 22 January 2016 – Accepted: 14 February 2016 – Published: 3 March 2016

Abstract. Variations in the stable oxygen isotope composition of atmospheric nitrate act as novel tools for studying oxidative processes taking place in the troposphere. They provide both qualitative and quantitative constraints on the pathways determining the fate of atmospheric nitrogen oxides ($NO + NO_2 = NO_x$). The unique and distinctive ^{17}O excess ($\Delta^{17}O = \delta^{17}O - 0.52 \times \delta^{18}O$) of ozone, which is transferred to NO_x via oxidation, is a particularly useful isotopic fingerprint in studies of NO_x transformations. Constraining the propagation of ^{17}O excess within the NO_x cycle is critical in polar areas, where there exists the possibility of extending atmospheric investigations to the glacial–interglacial timescale using deep ice core records of nitrate. Here we present measurements of the comprehensive isotopic composition of atmospheric nitrate collected at Dome C (East Antarctic Plateau) during the austral summer of 2011/2012. Nitrate isotope analysis has been here combined for the first time with key precursors involved in nitrate production (NO_x, O_3, OH, HO_2, RO_2, etc.) and direct observations of the transferrable $\Delta^{17}O$ of surface ozone, which was measured at Dome C throughout 2012 using our recently developed analytical approach. Assuming that nitrate is mainly produced in Antarctica in summer through the $OH + NO_2$ pathway and using concurrent measurements of OH and NO_2, we calculated a $\Delta^{17}O$ signature for nitrate on the order of (21–22 ± 3) ‰. These values are lower than the measured values that ranged between 27 and 31 ‰. This discrepancy between expected and observed $\Delta^{17}O(NO_3^-)$ values suggests the existence of an unknown process that contributes significantly to the atmospheric nitrate budget over this East Antarctic region. However, systematic errors or false isotopic balance transfer functions are not totally excluded.

1 Introduction

The search for ice core proxies to reconstruct past change of oxidative properties of the atmosphere is motivated by the need to simulate ozone and OH changes over preindustrial–industrial and glacial–interglacial timescales (Thompson, 1992; Wang and Jacob, 1998; Murray et al., 2014). Early ice core reconstructions of oxidants based on H_2O_2 (Sigg and Neftel, 1991) and HCHO (Staffelbach et al., 1991) measurements were hampered by the occurrence of post-depositional alteration of H_2O_2 and HCHO concentrations in the upper snowpack prior to preservation in the ice (Hutterli et

al., 2003). More recently, the ^{17}O excess ($\Delta^{17}O = \delta^{17}O - 0.52 \times \delta^{18}O$) of nitrate, a unique isotopic signature inherited from ozone via bimolecular chemical reactions in the atmosphere, has shown promise as a conserved proxy for past oxidant concentrations (McCabe et al., 2005; Alexander et al., 2004). The $\Delta^{17}O$ signal of nitrate reflects the relative importance of NO_x transformation mechanisms and recent studies suggest that the measurement of this isotopic signal in ice cores and ancient sediments may provide relevant information regarding the role of ozone in the overall oxidative capacity of the paleo-atmosphere (McCabe et al., 2007; Michalski et al., 2004, 2003; Savarino et al., 2007; Thiemens, 2006). Parallel studies of the nitrogen isotope ratios ($\delta^{15}N$) of nitrate in polar ice and snow suggest that this isotopic tracer may serve as a proxy for past variations in natural sources of atmospheric NO_x (Hastings et al., 2009, 2005; Jarvis et al., 2008). However, the chemical and physical factors governing the oxygen and nitrogen isotopic composition of atmospheric nitrate and its nitrogen oxide precursors are not fully understood (Alexander et al., 2009; Morin et al., 2009). This is particularly true in the polar troposphere, where the UV photolysis of trace species present in the snowpack or marine aerosols initiates complex boundary layer oxidation processes involving reactive halogen species (Bloss et al., 2010; Grannas et al., 2007; Wang et al., 2007) and results in distinctive $\Delta^{17}O$ and $\delta^{15}N$ signatures in atmospheric nitrate (Morin et al., 2007, 2008, 2012).

Here we present measurements of $\delta^{15}N$ and $\delta^{17}O$ and $\delta^{18}O$ isotopic composition of atmospheric nitrate collected at Dome C between November 2011 and January 2012. These measurements were conducted within the framework of the OPALE project (Oxidant Production over Antarctic Land and its Export; Preunkert et al., 2012), which has provided an opportunity to combine nitrate isotopic observations with a wealth of meteorological and chemical observations, including measurements of species involved in nitrate production (NO_x, O_3, OH, HO_2, RO_2, etc.). The primary objective of this study was to reconcile observations of $\Delta^{17}O$ for atmospheric nitrate at Dome C with quantitative predictions based on nitrate isotope mass balance and atmospheric chemistry parameters, a unique opportunity offered by the OPALE campaign.

2 Methods

2.1 Site description and scientific context

Dome C is situated 3233 m above sea level on the East Antarctic Plateau (75°06′ S, 123°23′ E), approximately 1100 km from the coastal research station Dumont d'Urville and 560 km from the Vostok station. Deep ice cores were extracted at Dome C in the framework of the European Project for Ice Coring in Antarctica (EPICA) covering approximately 800 000 years (EPICA community members, 2004) and Vostok covering the last 420 000 years (Petit et al., 1999). In parallel, studies aiming to understand the meteorological, chemical, and physical factors governing the variability in trace constituents preserved in the ice were initiated (Jourdain et al., 2008; Preunkert et al., 2008).

Although the Antarctic Plateau is extraordinarily dry, cold, and far removed from sources of anthropogenic emissions, first atmospheric measurements of oxidants conducted in 1998–1999 during the ISCAT (Investigation of Sulfur Chemistry in the Antarctic Troposphere) field campaign revealed a high level of photochemical activity. For example, the average summertime OH concentration (2×10^6 cm^{-3}) over the South Pole was found to be similar to that of the tropical marine boundary layer (MBL) (Mauldin et al., 2001). Unexpectedly high levels of nitric oxide (NO) were also detected, with concentrations 1 to 2 orders of magnitude higher than that typically observed in other remote regions (Davis et al., 2001). Model simulations revealed that the large OH concentrations observed at South Pole were a result of the elevated NO level, which catalyzes a rapid cycling of HO_2 to OH (Chen et al., 2004, 2001). The high concentrations of NO_x were also inferred to drive in situ photochemical production of ozone during the ISCAT campaign (Crawford et al., 2001). Surface ozone and NO_x measurements at Dome C suggest a similar level of enhanced oxidant production during November–January (Frey et al., 2013, 2015; Legrand et al., 2009).

The high levels of photochemical activity observed at South Pole and Dome C are now understood in terms of NO_x release from the snowpack (Honrath et al., 2000, 1999; Jones et al., 2001, 2000; Zhou et al., 2001). This process is initiated by the photolysis of nitrate, which can lead to large fluxes of NO_2, NO, and HONO from permanently sunlit snow (Anastasio and Chu, 2009; Grannas et al., 2007; Jacobi and Hilker, 2007; Legrand et al., 2014; Frey et al., 2013). Observed and modeled NO_x production rates are largely capable of explaining the high levels of photochemical activity observed on the Antarctic Plateau during spring (France et al., 2011; Liao and Tan, 2008; Wang et al., 2007) although detailed and speciation of nitrogen oxides chemistry remain largely unknown in this NO_x-rich/VOC-poor environment (Kukui et al., 2014; Frey et al., 2015; Legrand et al., 2014; Davis et al., 2008).

2.2 High-volume sampling

Bulk atmospheric samples were collected at Dome C on glass fiber filters using a high-volume air sampler (HVAS), which was installed on a platform 1 m above the ground. The HVAS was run by applying an average STP (standard temperature and pressure) flow rate of 0.7 m^3 min^{-1} that ensures the collection of a sufficient amount of nitrate for isotopic analysis. The atmospheric NO_3^- collected on glass fiber filters represents the sum of atmospheric particulate NO_3^- (pNO_3^-) and gaseous nitric acid (HNO_3) (Frey et al., 2009). Eleven HVAS

samples were obtained during the OPALE campaign (from November 2011 to January 2012). After each collection period, filters were removed from the HVAS and placed in clean 50 mL centrifuge tubes, which were sealed in plastic bags and stored at −20 °C. Upon arrival at our laboratory in Grenoble, atmospheric filter samples were extracted in 40 mL of ultra-pure water via centrifugation using Millipore Centricon® filter units. Nitrate concentration was then determined for each filter extract solution using a colorimetric technique (Frey et al., 2009).

2.3 Ozone collection

The nitrite-coated filter technique for ozone isotope analysis has been described in detail in Vicars et al. (2012) and Vicars and Savarino (2014). The principle of ozone collection underlying this technique is the filter-based chemical trapping of ozone via aqueous-phase reaction with nitrite (Adon et al., 2010; Geyh et al., 1997; Koutrakis et al., 1993; Krzyzanowski, 2004):

$$NO_2^- + O_3 \rightarrow NO_3^- + O_2. \quad \text{(R1)}$$

By coupling this routine ozone measurement technique with recent analytical developments in the $\Delta^{17}O$ analysis of nanomole quantities of nitrate (Kaiser et al., 2007), the ^{17}O excess transferred by one of the two O_3 terminal atoms through bimolecular chemical reactions, denoted $\Delta^{17}O(O_3)_{term}$, as well as ozone's bulk $\Delta^{17}O$ value, denoted $\Delta^{17}O(O_3)_{bulk}$ ($= 2/3\ \Delta^{17}O(O_3)_{term}$ since all ^{17}O excess is located at the two O_3 terminal atoms; Bhattacharya et al., 2008; Janssen and Tuzson, 2006), can be inferred from the oxygen isotopic composition of the nitrate produced via R1 within the coated filter matrix.

Ambient ozone collections were performed using an active air sampler consisting of 1/4 in. Teflon® (PFA) tubing connecting three main sampler components: (i) a standard low-volume vacuum pump (Welch®, model 2522C-02) equipped with a volume counter and needle valve (or flow meter) for flow rate regulation, (ii) a closed PFA filter holder assembly (Savillex®) containing a pre-coated 47 mm glass fiber sampling substrate (Whatman®, GF/A type), and (iii) an open-faced PFA filter holder assembly containing a 47 mm PTFE membrane filter (Zylon®, 5 µm pore size) for the removal of particulate species upstream of the coated filter. Glass fiber sampling substrates were coated prior to sample collection with 1 mL of a nitrite-based ozone sampling solution (0.1 M $NaNO_2$, 0.05 M K_2CO_3, 0.1 M glycerol) (Koutrakis et al., 1993), allowed to dry at 75 °C for approximately 10 min, and then stored frozen in the dark in individual plastic PetriSlide™ containers (Millipore®). Samples were collected by loading pre-coated filters into the sampling filter holder, which was then connected to the prefilter (upstream) and needle valve/pump (downstream) and covered in aluminum foil to limit light exposure, a step that is necessary to limit the blank production rate during sample collection (Vicars et al., 2012). Air was then pumped through the sampling system at a target flow rate of 3.0 L min^{-1}.

Sampling was conducted during the OPALE campaign (December 2011–January 2012) from a climate-controlled shelter, and a total of 28 samples were collected. However, due to difficulties in the application of our analytical technique to the unique environmental conditions encountered in Antarctica, the results obtained from these samples were inconclusive (i.e., unrealistic variability) due to the lack of light protection of the filter holder (Vicars et al., 2012, 2013). Sampling and isotopic analysis of ozone was therefore repeated in 2012, and a complete annual record of $\Delta^{17}O(O_3)$ was obtained ($n = 60$). Procedural filter blanks were also collected at regular intervals and were subjected to all of the same preparation, storage, handling, and analytical procedures as field samples. After sample collection, filter samples and procedural blanks were returned to their containers, which were covered in aluminum foil and stored at −20 °C before processing and analysis.

Filter samples were extracted in 18 mL of deionized water (18.2 MΩ, hereafter referred to as "MQ water"). In order to remove the excess (i.e., unreacted) nitrite reagent from the sample extracts, the solutions were treated with 1 mL of a 1 M sulfamic acid solution and then neutralized with a corresponding addition of high-purity sodium hydroxide (Granger and Sigman, 2009; Vicars et al., 2012). Extract solutions were then filtered via centrifugation using Millipore Centricon® assemblies. The nitrate extracted from the coated filter samples was then subjected to isotopic analysis, as described in the following section.

2.4 Isotopic analysis

The comprehensive isotopic composition of nitrate ($^{15}N/^{14}N$, $^{17}O/^{16}O$, $^{18}O/^{16}O$) was measured on a Finnigan™ MAT253 isotope ratio mass spectrometer (IRMS), equipped with a GasBench II and coupled to an in-house-built nitrate interface (Morin et al., 2009). Nitrate in both the nitrite-coated filter and aerosol sample extracts was prepared for isotopic analysis by conversion to N_2O via the bacterial denitrifier method (Casciotti et al., 2002; Kaiser et al., 2007; Michalski et al., 2002; Sigman et al., 2001). The detailed analytical procedure has been described elsewhere (see Morin et al., 2009) and is briefly presented here.

Denitrifying bacteria (*Pseudomonas aureofaciens*) were cultured in nitrate-amended soy broth and incubated for 5 days in stoppered glass bottles. Bacterial cultures, after concentration by centrifugation and resuspension, were dispensed as 2 mL aliquots into 20 mL glass vials, which were then crimped and purged with helium for 3 h. Approximately 100 nmol of sample nitrate was then injected into the purged vials and conversion of the sample nitrate to nitrous oxide (N_2O) via bacterial denitrification was allowed to proceed overnight. The N_2O sample was then cryo-focused in a liquid nitrogen trap and introduced into a gold furnace where

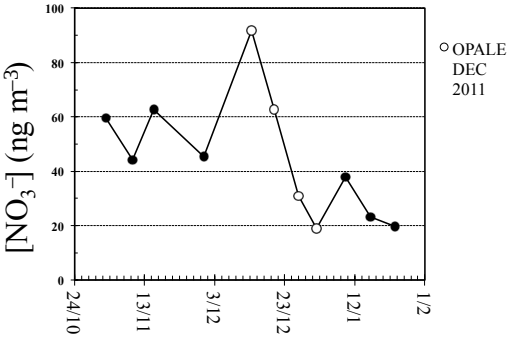

Figure 1. Atmospheric nitrate concentrations observed between November 2011 and January 2012. The samples collected during the intensive measurement period (December 2011–January 2012) are indicated with open circles.

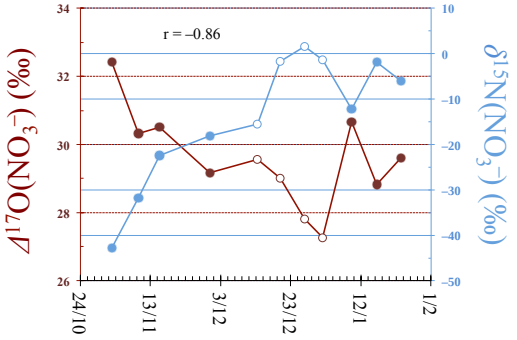

Figure 2. $\Delta^{17}O$ (primary y axis) and $\delta^{15}N$ (secondary y axis) of atmospheric nitrate collected between November 2011 and January 2012. The samples collected during the intensive measurement period (December 2011–January 2012) are indicated with open symbols.

it was thermally decomposed at 900 °C into O_2 and N_2. Following separation via gas chromatography, the O_2 and N_2 gas samples were directed into the ionization chamber of the IRMS. All analytical steps were identically performed on nitrate isotopic standards and their equimolar mixtures (International Atomic Energy Agency USGS 32, USGS 34, and USGS 35), which were prepared in an identical background matrix as the samples. Individual analyses were normalized through comparison with these three nitrate reference materials (Coplen, 2011; Werner and Brand, 2001). All isotopic enrichment values for nitrate are reported relative to VSMOW and air N_2 for oxygen and nitrogen, respectively. The overall accuracy of the method is estimated as the standard deviation of the residuals from the linear regression between the measured reference materials and their expected values. For the results reported here, the average uncertainties obtained for $\delta^{18}O$, $\Delta^{17}O$, and $\delta^{15}N$ were 1.6, 0.5, and 1.0 ‰, respectively.

2.5 Complementary measurements

Concurrent chemical measurements were conducted at Dome C during the campaign include HONO (Legrand et al., 2014), HO_x ($= OH + HO_2 + RO_2$) radicals (Kukui et al., 2014), O_3 (Legrand et al., 2016) and NO and NO_2 (Frey et al., 2015). Photolysis rate coefficients and meteorological parameters were also recorded.

3 Results and discussion

3.1 Isotope ratios of ozone and atmospheric nitrate

Atmospheric nitrate concentrations observed at Dome C during the campaign are presented in Fig. 1, and the corresponding nitrate $\Delta^{17}O$ and $\delta^{15}N$ values in Fig. 2. Atmospheric nitrate concentrations ranged between 20 and 90 ng m^{-3}, with the maximum values occurring in mid-December 2011, concurrent with the period of intensive of atmospheric sampling of the OPALE field campaign. These values are in good agreement with those observed during the 2007–2008 and 2009–2010 field studies conducted at Dome C by Frey et al. (2009) and Erbland et al. (2013), respectively.

$\Delta^{17}O$ values for atmospheric nitrate ranged between 27.3 and 32.4 ‰, and those for $\delta^{15}N$ between −42.8 and 1.7 ‰. The observed strongly depleted $\delta^{15}N(NO_3^-)$ values are in good agreement with those previously reported and having unambiguously attributed to the transformation of local snowpack NO_x emissions via photochemistry in the boundary layer, which led to peaks in atmospheric nitrate concentration during the period from October to December (Erbland et al., 2013). As seen in Fig. 2, variations in $\Delta^{17}O$ and $\delta^{15}N$ were negatively correlated (r value of −0.86) and again show similar amplitude and phase to those reported in previous studies (Erbland et al., 2013; Frey et al., 2009).

A time series showing the year-round record of $\Delta^{17}O(O_3)_{bulk}$ at Dome C in 2012 is presented in Fig. 3. $\Delta^{17}O(O_3)_{bulk}$ averaged 24.9 ± 1.9 ‰, derived from $\Delta^{17}O(O_3)_{term}$ values of 37.4 ± 1.9 ‰. As shown in Fig. 4, these $\Delta^{17}O(O_3)_{bulk}$ values are consistent with those observed in Grenoble (France), as well as with measurements conducted along a latitudinal transect from 50° S to 50° N in the Atlantic Ocean (Vicars and Savarino, 2014). Although the $\Delta^{17}O(O_3)_{bulk}$ seasonal cycle reveals some interesting features, like the winter maximum, probably in response of the permanent winter darkness and stratospheric air mass intrusions, a complete description is beyond the scope of the present paper. What should be kept in mind here is the quite stable $\Delta^{17}O(O_3)_{bulk}$ value close to 26 ‰ that can be considered as representative of the OPALE campaign held in November–January.

3.2 Nitrate isotope mass balance

The availability of a large database of trace chemical species measurements at Dome C during a portion of the OPALE field campaign (December 2011) offers a unique opportu-

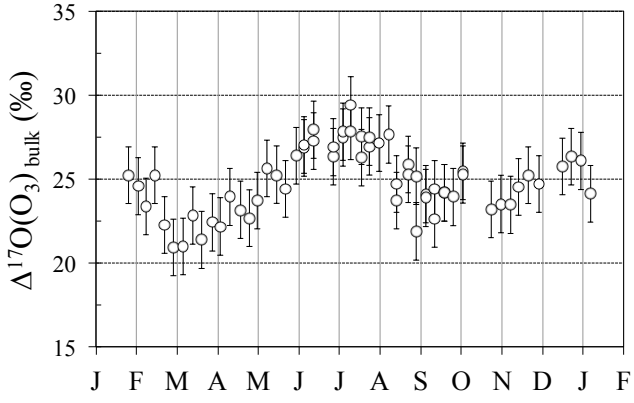

Figure 3. $\Delta^{17}O(O_3)_{bulk}$ values for the 60 ambient air samplings done at Dome C throughout 2012. Vertical error bars refer to the total uncertainty estimated for the technique (±1.7 ‰).

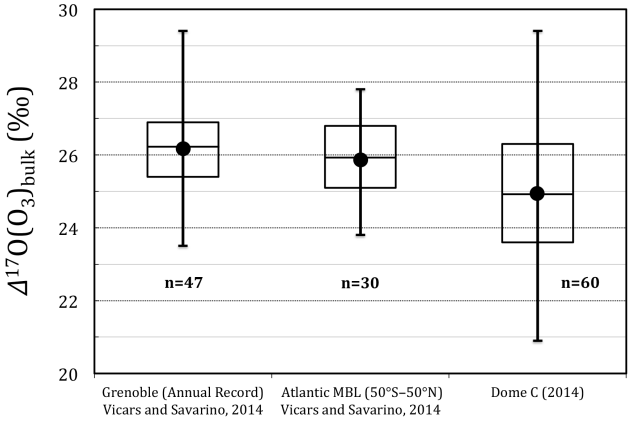

Figure 4. Comparison of $\Delta^{17}O(O_3)_{bulk}$ values obtained at Dome C with those previously reported by Vicars and Savarino (2014) at other sites. Box plots indicate the interquartile range (box) and the median (line), maximum, and minimum values. The mean value is denoted by a circle.

nity to compare observed $\Delta^{17}O(NO_3^-)$ values in the atmosphere to ones calculated from concurrent observations. As discussed at length in recent studies (for example, by Morin et al., 2011, and Vicars et al., 2013), the ^{17}O-excess transfer functions associated with the various nitrate production pathways (i.e., $\Delta^{17}O(NO_3^-)_i$ values) can be estimated as a function of the $\Delta^{17}O$ of nitrate precursor gases (i.e., NO_x, O_3, OH, etc.) using mass balance calculations that trace the origin of oxygen atoms transferred during the chemical transformation of NO_x in the atmosphere. All atmospheric nitrate production channels involve either NO_2 or a NO_x reservoir species derived from NO_2 (e.g., N_2O_5). The first step in determining the $\Delta^{17}O$ signature of each pathway is therefore a quantitative assessment of the steady-state $\Delta^{17}O$ value of NO_2, which is typically calculated as a function of the $\Delta^{17}O$ value of O_3 and the reaction dynamics involved in the conversion of NO to NO_2. As Dome C in summer is permanently under sunlight, photochemical inter-conversion of NO_x continues:

$$NO_2 + h\nu \rightarrow NO + O, \quad \text{(R2)}$$

$$NO + O_3 \rightarrow NO_2, \quad \text{(R3)}$$

$$NO + HO_2/RO_2 \rightarrow NO_2. \quad \text{(R4)}$$

At photochemical steady state (i.e., R2–R4 being faster than NO_2 net sink reactions), an assumption that can be reasonably applied throughout the day at Dome C during summer, we have (Morin et al., 2011)

$$\Delta^{17}O(NO_2) = \alpha \times \left(1.18 \times \Delta^{17}(O_3)_{bulk} + 6.6\right), \quad (1)$$

where the term in bracket represents the laboratory-deduced anomaly transfer function of the $NO + O_3$ reaction (Savarino et al., 2008), $\Delta^{17}O(O_3)_{bulk}$ the ^{17}O excess of the bulk O_3 and α represents the fraction of the atmospheric NO_2 reservoir that has been produced through oxidation by O_3 rather than HO_2 / RO_2 at photochemical equilibrium (Alexander et al., 2009; Michalski et al., 2003; Morin et al., 2011; Röckmann et al., 2001):

$$\alpha = \frac{k_{NO+O_3}[NO][O_3]}{k_{NO+O_3}[NO][O_3] + k_{NO+HO_2}[NO][HO_2]^*}, \quad (2)$$

with $[HO_2]^* = [HO_2] + [RO_2]$.

It is important to note here that Eqs. (1) and (2), although established under the NO_x steady-state approximation, are independent of NO_2 concentration, for which a bias in measurement cannot be ruled out. Indeed, as discussed by Frey et al. (2013, 2015), bias in NO_2 measurements is suspected partly because it remains difficult to explain the observed ratio of NO_2 / NO, which is systematically higher (up to a factor of 7) than predicted by calculations made by assuming photochemical steady state considering the NO_2 photolysis and reaction of NO with O_3, HO_2 / RO_2 and BrO. Equation (2) also assumes that $[HO_2]^*$ is predominantly formed by the reaction $H + O_2$ and $R + O_2$ during the OPALE campaign (Kukui et al., 2014), resulting in the formation of $[HO_2]^*$ devoid of any significant ^{17}O excess (Morin et al., 2011). Using OPALE measurements of NO, O_3, OH and HO_2 / RO_2 (Frey et al., 2015; Kukui et al., 2014), along with temperature dependent reaction kinetics data obtained from Atkinson et al. (2004), we have calculated the diurnally mass-averaged trend in α for the month of December 2011 at Dome C. Measurements of $\Delta^{17}O(O_3)_{bulk}$ at Dome C during the OPALE campaign averaged 25 ± 2 ‰, corresponding to $\Delta^{17}O(O_3)_{term}$ values of 37 ± 2 ‰ (Fig. 4). Samples collected in December indicate $\Delta^{17}O(O_3)_{bulk}$ values close to 26 ‰ ($\Delta^{17}O(O_3)_{term} = 3/2\Delta^{17}O(O_3)_{bulk} = 39$–40 ‰, Fig. 3), and we have therefore adopted a $\Delta^{17}O(O_3)_{term}$ value of 40 ‰ in the subsequent mass balance calculations, in good agreement with the predicted value from a 1-D at-

Table 1. Example of mass balance calculation of $\Delta^{17}O$ for 19 December 2011 at 15:45 local time (UTC + 8 h).

Conditions for 19 December 2011, 15:45 $OH = 3.96 \times 10^6$ molecules cm^{-3}		[a]Median rate in 10^5 molecules cm^{-3} s^{-1}	$\Delta^{17}O_i^c$ in ‰
Net sources of OH			
P1	$HONO + h\nu \rightarrow OH + NO$	5.1[b]	32
P2	$H_2O_2 + h\nu \rightarrow 2\ OH$	1.7	2
P3	$O_3 + h\nu + H_2O \rightarrow 2\ OH$	0.6	20
P4	$CH_3OOH + h\nu \rightarrow HO_2 + OH$	0.3	0
Recycling $RO_2 \rightarrow OH$			
P5	$NO + HO_2 \rightarrow NO_2 + OH$	7.7	0
P6	$HO_2 + O_3 \rightarrow OH + 2O_2$	0.4	0
Net sink of OH			
L1	$CO + OH \rightarrow HO_2 + CO_2$	6.3	
L2	$CH_4 + OH \rightarrow CH_3O_2 + H_2O$	2.6	
L2	$HCHO + OH \rightarrow HO_2 + CO$	0.8	
L4	$CH_3CHO + OH \rightarrow CH_3CO_3$	0.9	
L5	$O_3 + OH \rightarrow HO_2 + O_2$	0.6	
L6	$H_2 + OH + O_2 \rightarrow HO_2 + H_2O$	0.60	
L7	$CH_3OOH + OH \rightarrow CH_3O_2 + H_2O$	0.5	
L8	$H_2O_2 + OH \rightarrow HO_2 + H_2O$	0.3	
Net OH losses			
L9	$NO_2 + OH \rightarrow HNO_3$	3.9	
L10	$NO + OH \rightarrow HONO$	0.6	
L11	$OH + RO_2 \rightarrow$ products	0.5	
L12	$OH + RO_2NO_2 \rightarrow$ products	0.6	
L13	$OH + HONO \rightarrow NO_2 + H_2O$	0.2	
L14	$OH + HNO_3 \rightarrow H_2O + NO_3$	0.0	
Isotope exchange			
E_1	$HQ + H2O \Longleftrightarrow HO + H2Q$	24.3	
NO_2 main source			
N1	$NO + O_3 \rightarrow NO_2 + O_2$	27.0	37
^{17}O-excess NO_2			
$\alpha = (N1/N1 + P5)$	0.78		
$\Delta^{17}O(NO_2)$		29	
^{17}O-excess OH			
$\Delta^{17}O(OH)_{prod} = (\sum P_i \cdot \Delta^{17}O_i)/\sum P_i$		5.8	
$\beta = \sum L_i/(\sum L_i + E_1)$	0.43		
$\Delta^{17}O(OH)$		2.5	

[a] Production rates obtained from a 0-D box model (see Kukui et al., 2014, for details). [b] HONO production rate divided by a factor of 4 to balance the HO_x radical budget (see Kukui et al., 2014, and Legrand et al., 2014, for justification). [c] HONO is assumed to be formed by the photodissociation of nitrate in snow. $\Delta^{17}O(NO_3^-)_{snow}$ is therefore assigned to HONO. The rest of the ^{17}O-excess transfer (i.e., P2 to P6 and N1) follows the rules established in Morin et al. (2011) and $\Delta^{17}O(O_3)_{bulk} = 26$ ‰.

mospheric model (Zahn et al., 2006). The diurnally mass average of $\Delta^{17}O(NO_2)$ calculated using a $\Delta^{17}O(O_3)_{bulk}$ value of 26 ‰ and Eq. (2) is shown in Fig. 5. No trend is observed during the OPALE campaign, and on average the predicted value is $\Delta^{17}O(NO_2) = 31 \pm 2$ ‰ throughout December, corresponding to average α value of 0.83. In other words, at steady state, the concentrations of O_3 and HO_2^* measured during OPALE predicts that around 83 % of NO_2 is formed

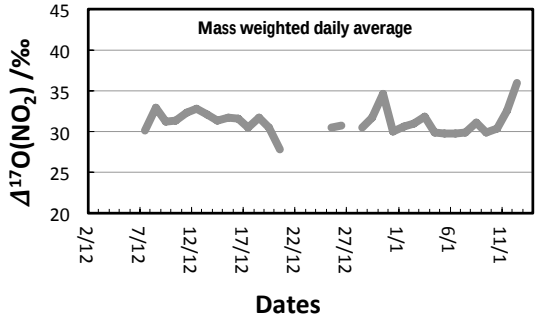

Figure 5. Quantitative assessment of the daily averaged trend in the $\Delta^{17}O$ of NO_2 at Dome C during December 2011–January 2012 derived from concurrent measurements of ozone, NO, and HO_2 / RO_2.

via R3 (see also Table 1). In the absence of the α dilution effect introduced by the HO_2^* reaction, $\Delta^{17}O(NO_2)$ would equal 37 ‰, a value 8 ‰ lower than an estimation obtained from modeling only NO_x–O_3 chemistry at standard temperature and pressure (Michalski et al., 2014). This difference is essentially explained by the use of different $\Delta^{17}O(O_3)_{bulk}$ (32 ‰ in Michalski's simulation, 26 ‰ for our observations), which possibly corresponds to different conditions of the two studies.

By accounting for the origin of the oxygen atom transferred during the conversion of NO_2 to nitrate, the $\Delta^{17}O$ signature of the nitrate produced through different reaction mechanisms can be calculated. For summer conditions at Dome C, it is reasonable to assume that the dominant atmospheric nitrate formation pathway is the gas-phase association of NO_2 and the OH radical (Alexander et al., 2009):

$$NO_2 + OH + M \rightarrow HNO_3 + M, \quad \text{(R5)}$$

leading to the following ^{17}O-excess mass balance (Michalski et al., 2003; Morin et al., 2011):

$$\Delta^{17}O\left(NO_3^-\right) = \frac{2}{3}\Delta^{17}O\left(NO_2\right) + \frac{1}{3}\Delta^{17}O\left(OH\right). \quad (3)$$

In order to predict the $\Delta^{17}O$ value of the nitrate produced through R5 by mass balance, the isotopic composition of tropospheric OH must be known. The OH radical participates in a rapid isotopic exchange with atmospheric water vapor, which represents a very large oxygen reservoir relative to OH, with a $\Delta^{17}O$ that is negligible compared to ozone or nitrate (Luz and Barkan, 2010). This exchange tends to erase the ^{17}O excess of OH under humidity and temperature conditions typical of the midlatitudes (Dubey et al., 1997); therefore, the $\Delta^{17}O$ of OH is normally assumed to be zero in modeling studies applied to these regions. As discussed by Morin et al. (2007), this assumption of $\Delta^{17}O(OH) = 0$ is not valid under the low-humidity conditions encountered in the polar atmosphere. The degree of isotopic equilibration between OH and H_2O can be determined as a function of the relative rates of the isotope exchange reaction and the main OH sink reactions:

$$\beta = \frac{L}{L + k_{H_2O+OH}[H_2O]}, \quad (4)$$

where L represents the total chemical loss rate of OH. β is the factor relating the initial $\Delta^{17}O$ transferred to OH upon its formation, denoted $\Delta^{17}O(OH)_{prod}$, to its steady-state $\Delta^{17}O$ value (Morin et al., 2007):

$$\Delta^{17}O(OH) = \beta \times \Delta^{17}O(OH)_{prod}. \quad (5)$$

In plain words, Eqs. (4)–(5) predict that when the isotopic exchange reaction dominates over OH chemical losses (i.e., $\beta \ll 1$), the steady-state $\Delta^{17}O$ value of OH will be equal to that of water (i.e., $\Delta^{17}O \approx 0$ ‰). Conversely, when water vapor concentrations are low and the rate of chemical loss is large relative to the rate of the isotopic exchange, $\Delta^{17}O(OH) = \Delta^{17}O(OH)_{prod}$. Kukui et al. (2014), using a Master Chemical Mechanism box model, constrained by the OPALE meteorological conditions and concurrent chemical observations, give the rate of the OH chemical sources and sinks. NO_2 as measured by Frey et al. (2015) represents at most only ca. 10 % (equivalent of ca. 1 ‰) of the total sink of OH, which is predominantly dominated by reactions with CO, CH_4, aldehydes and to a lesser extent by reactions with O_3, H_2, and NO. Thus, the possible overestimation of NO_2 concentration has only a minor effect on β calculation and is well embedded within the total uncertainty of such calculation. To assess the value of $\Delta^{17}O(OH)$, we have computed β for the conditions found during the OPALE campaign using the same 0-D box model that is used to evaluate the budget of OH and RO_2 during the OPALE campaign (see Kukui et al., 2014, and Table 1) and used the exchange kinetic rates given in Dubey et al. (1997). The absolute water vapor concentration is deduced from relative humidity and temperature measurements using Bolton (1980) (i.e., $P_{water} = 6.112 \times e^{\frac{(17.67\times(T-273)}{T-29.5}}$, with P_{water} in hPa and T in K). The results of this calculation (Fig. 6) indicate that β varies between 0.70 ± 0.10 (1σ) and 0.30 ± 0.10 from midnight to noon for conditions prevailing during the OPALE campaign, suggesting that, on a daily average basis, approximately 43 % of the $\Delta^{17}O$ value originally present in OH is preserved from exchange with H_2O, consistent with estimates for an Arctic site described by Morin et al. (2007).

The value of $\Delta^{17}O(OH)_{prod}$ is more difficult to assess because of the interplay between HO and HO_2, and the different sources involved in OH formation. In the NO_x-rich atmosphere at Dome C in summer, the $O(^1D) + H_2O$ reaction forming OH is a minor reaction pathway. When multiple pathways are involved in the production of OH, $\Delta^{17}O(OH)_{prod}$ can be estimated by a simple isotope mass balance equation where $\Delta^{17}O(OH)_{prod} = \sum_i P_i \times \Delta^{17}O_i$, with P_i the relative production rate of the ith reaction pathway with respect to the total production rate and $\Delta^{17}O_i$ its

Table 2. Comparison of measured and calculated $\Delta^{17}O(NO_3^-)$ values.

Sampling period	Measured	Calculated			
		α constrained by observations $\Delta^{17}O(OH)^*$ based on HO_x budget	$\alpha = 1$ $\Delta^{17}O(OH)^*$ based HO_x budget	α constrained by observations $\beta = 1$	α constrained by observations $\Delta^{17}O(OH)$ based on observed HONO
10–16 Dec	29.6	21.9	25.6	22.6	27.0
16–23 Dec	29.0	21.0	25.6	21.7	26.3
23–30 Dec	27.8	21.6	25.4	22.0	25.7
30 Dec–2 Jan	27.3	21.5	25.3	22.4	24.9

* HONO production rate divided by a factor of 4 to balance the HO_x radical budget (see Kukui et al., 2014, and Legrand et al., 2014, for justification).

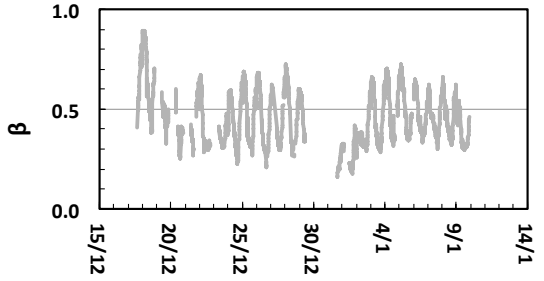

Figure 6. December 2011 time series for β, the fraction of the ^{17}O excess originally associated with the OH radical that is preserved against isotopic exchange with water.

associated ^{17}O excess (Morin et al., 2011). Observations at Dome C during the OPALE campaign indicate that the photolysis of HONO and the $HO_2 + NO$ reaction may represent the most significant sources of OH at Dome C during the period of seasonal snowpack emissions (Kukui et al., 2014). However, the measurement of HONO (around few 10 pmol mol^{-1}) during OPALE, probably biased by HO_2NO_2 interference (Legrand et al., 2014), is incompatible with the HO_x ($= OH + HO_2 / RO_2$) radical budget. Best agreement is achieved when HONO at Dome C is assumed to originate from snow emissions with the emission strength evaluated by Legrand et al. (2014). Using a 1-D model, Kukui et al. (2014) show that the concentrations of HONO corresponding to about 20–30 % of measured HONO are consistent with those calculated from the budget analysis of OH radicals with the concentrations of NO_2 either calculated from NO measurements assuming PSS or observed by Frey et al. (2015). Therefore, the production of OH by HONO photolysis is consequently adjusted and the 0-D box model (Kukui et al., 2014) is used to calculate all other production rates of OH. Note that, even when lowering HONO to 20–30 % of the measured values, this species remains the major primary source of radicals at Dome C. Applying the isotope ^{17}O-excess transfer (Morin et al., 2011) and the OH_{prod} isotope mass balance, $\Delta^{17}O(OH)_{prod}$ on average equals 5 ± 2 ‰ (1σ). Because the major process leading to the emission of HONO from the snowpack is the photolysis of nitrate, which possesses a $\Delta^{17}O$ value of approximately 32 ‰, both in the snow "skin layer" (Erbland et al., 2013) and in the top 10 cm of snow (Frey et al., 2009), we have assumed that $\Delta^{17}O(HONO)_{atm} = \Delta^{17}O(NO_3^-)_{snow}$ as both oxygen atoms of HONO can be tracked back to the nitrate. An example of the isotope mass balance calculation is given in Table 1. Figure 7 shows the diurnally integrated average of the $\Delta^{17}O(OH)$. $\Delta^{17}O(OH)$ varies in a narrow range, between 1 and 3 ‰. An estimation of the $\Delta^{17}O$ signature for the $NO_2 + OH$ channel, $\Delta^{17}O(NO_3^-)_{R2}$, that accounts for the ^{17}O excess carried by the OH radical results in values ranging between 20 and 23 ‰. Averaging over the same time period as the nitrate atmospheric sampling, diurnally integrated average $\Delta^{17}O(NO_3^-)$ values of 21–22 ‰ $\pm$ 3 ‰ can be estimated for December (Table 2). These values are 6–8 ‰ lower than the observed atmospheric values for $\Delta^{17}O(NO_3^-)$ (27–30 ‰ during OPALE, Fig. 2 and Table 2). The source of discrepancy between observed and modeled $\Delta^{17}O(NO_3^-)$ during OPALE is presently unknown, but we note that such underestimation of the modeled $\Delta^{17}O(NO_3^-)$ versus the observed $\Delta^{17}O(NO_3^-)$ was also pointed out in 3-D modeling of the nitrate $^{17}O_{excess}$ (Alexander et al., 2009). A critical evaluation may nevertheless offer some clues.

4 Discussion

4.1 Alternative sources of NO_2

A possible explanation for the underestimation of $\Delta^{17}O(NO_3^-)$ involves halogen chemistry in the troposphere over the Antarctic Plateau (Bloss et al., 2010; Morin et al., 2008). Reactive halogen oxides (XO = BrO, ClO, IO, etc.) are produced through the reaction of halogen radicals (X) with ozone, a pathway that plays an important role in the catalytic process responsible for ozone depletion events (ODEs) observed in the Arctic boundary layer since the

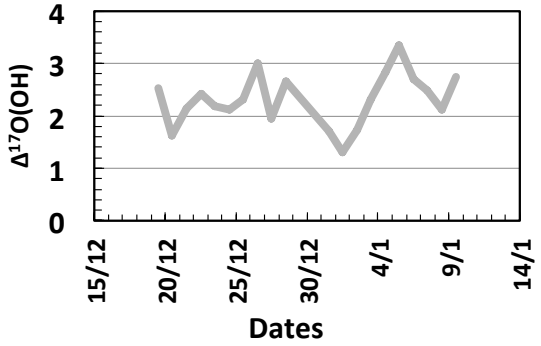

Figure 7. Same as Fig. 5 but for Δ^{17}O of OH.

1980s (Fan and Jacob, 1992; Simpson et al., 2007):

$$X + O_3 \rightarrow XO + O_2. \quad \text{(R6)}$$

In terms of the chemical budget of NO_x, the impact of XO can occur via two chemical mechanisms (see Sect. 4.2 for the second mechanism involving the formation of halogen nitrate, $XONO_2$). First, XO can oxidize NO to NO_2, a pathway that competes with the $NO + O_3$ and $NO + HO_2 / RO_2$ reactions in terms of NO oxidation:

$$XO + NO \rightarrow X + NO_2. \quad \text{(R7)}$$

For conditions typical of the Antarctic boundary layer, 1 pmol mol^{-1} of XO has roughly the same chemical activity as 4 nmol mol^{-1} of ozone in terms of NO oxidation (Atkinson et al., 2007). Therefore, when halogen oxides are present at relevant levels, R7 can result in concentrations of NO_2 that are higher than that predicted from the balance between NO_2 destruction via photolysis and production through the reaction of NO with O_3 or HO_2 / RO_2 (i.e., the extended Leighton mechanism):

$$\frac{[NO_2]}{[NO]} = \frac{k_{NO+O_3}[O_3] + k_{NO+HO_2}[HO_2] + k_{NO+RO_2}[RO_2] + k_{NO+XO}[XO]}{j_{NO_2}}. \quad (6)$$

The involvement of XO in the NO_x cycle at Dome C would have important implications for the Δ^{17}O of atmospheric nitrate. The production of halogen oxide radicals proceeds through a direct transfer of a terminal oxygen atom from ozone to the XO product (Zhang et al., 1997). Therefore, it is expected that the Δ^{17}O of XO is equal to $\Delta^{17}O(O_3)_{term}$, which means that the reaction of NO with XO is roughly equivalent to the $NO + O_3$ reaction in terms of Δ^{17}O transfer to NO_2 (note that the $NO + XO$ transfer is greater than $NO + O_3$ as, in the later case, part of the central O_3 atom participates in the reaction). The participation of XO species in the oxidation of NO thus leads to a greater Δ^{17}O transfer to NO_2 by effectively increasing the value of α. However, on the Antarctic Plateau, BrO did not exceed 2–3 pmol mol^{-1} during the OPALE campaign (Frey et al., 2015). Including BrO chemistry would only increase α by 2 % (due to the specific form of $\alpha \equiv 1/(1+x)$), which is too low to significantly influence $\Delta^{17}O(NO_2)$ and ultimately $\Delta^{17}O(NO_3^-)$. In the absence of measurements of other halogens we cannot completely rule out a role of the halogen chemistry there. However, even with $\alpha = 1$, its maximum but unrealistic value due to the high concentration of HO_2, $\Delta^{17}O(NO_3^-)$ would reach the range of 23–25 ‰, in better agreement with the observations but still significantly lower. Similarly, in the event of a non-isotopic steady state of NO_2 (Michalski et al., 2014), it is very unlikely that $\Delta^{17}O(NO_2)$ could reach values greater than its primary snow nitrate source (i.e., $\Delta^{17}O(NO_2) > \Delta^{17}O(NO_3^-)_{snow} = 30$–35 ‰ in summer at Dome C; Erbland et al., 2013; Frey et al., 2009), still leaving the predicted $\Delta^{17}O(NO_3^-)$ underestimated with respect to atmospheric observations.

4.2 Alternative oxidation pathways of NO_2

Considering R5 as the main source of HNO_3, an alternative approach is to consider that OH bears a higher Δ^{17}O than the estimate calculated previously. Assuming a β of 1, which seems again unrealistic, will increase $\Delta^{17}O(NO_3^-)$ by 1 ‰ at most (Table 2), still insufficient to explained atmospheric observations as $NO + HO_2$ remain a major source of OH, independent of the assumed β.

Alternatively, if measured HONO concentrations are considered instead of those assumed to constrain by the HO_x budget (i.e., 4 times lower than measured), average $\Delta^{17}O(NO_3^-)$ values of 23–24 ‰ are calculated (Table 2), again systematically lower than the observed range of 27–30 ‰. However, given the significant uncertainty surrounding the isotopic composition of HONO and its relative contribution to total OH production at Dome C, it is not possible to make a firm conclusion in this regard.

Therefore, neither the common sources of NO_2 nor the daytime formation of HNO_3 seems to be able to explain the high $\Delta^{17}O(NO_3^-)$ values of atmospheric nitrate observed at Dome C in summer. When this observation is taken together with the high NO_2 / NO ratio observed by Frey et al. (2013, 2015) during two summer seasons at Dome C, clearly our current understanding of the NO_x chemistry on the Antarctic Plateau seems to be incomplete.

There are several other processes that possibly account for the disagreement between the measurements and mass balance calculations. Indeed, in addition to its impact on NO_x cycling through the R7 pathway, an increasing body of evidence points towards reactive halogen chemistry as a major NO_x sink and source of nitrate via the production and subsequent hydrolysis of XNO_3 species (Sander et al., 1999; Savarino et al., 2013; Vogt et al., 1996):

$$XO + NO_2 + M \rightarrow XNO_3 + M, \quad \text{(R8)}$$

$$XNO_3 + H_2O_{(liquid)} \rightarrow HNO_{3(aq)} + HOX. \quad \text{(R9)}$$

A critical analysis of the CHABLIS data led Bauguitte et al. (2012) to conclude that R8–R9 pathway exerted predominant control over the chemical loss rate of NO_x during the campaign, despite the significant uncertainties involved in the parameterization of the uptake processes (Finlayson-Pitts, 2009). This implies that XNO_3 uptake may also represent a significant source of nitrate at Dome C should halogen oxide radicals (XO) be present at the required concentration. Experimental (Gane et al., 2001) and theoretical (McNamara and Hillier, 2001) studies suggest that the oxygen atom initially associated with XO combines with the N atom of NO_2 to form nitrate, thus transferring the isotopic signature of both XO and NO_2. The specific $\Delta^{17}O$ value induced by XNO_3 hydrolysis can thus be expressed as follows (Morin et al., 2007):

$$\Delta^{17}O\left(NO_3^-\right)_{R6} = \frac{2}{3}\Delta^{17}O\left(NO_2\right) + \frac{1}{3}\Delta^{17}O(O_3)_{term}, \quad (7)$$

efficiently bypassing the OH ^{17}O-excess budget. Through consideration of the increased $\Delta^{17}O$ transfer associated with R8, the observations of $\Delta^{17}O(NO_3^-)$ during December can be reconciled with the values calculated by mass balance if approximately 10–20 % of total nitrate production is assumed to occur via XNO_3 hydrolysis. However, no sufficient halogen concentration has been observed on the Antarctic Plateau to sustain such a chemical pathway, but we note that chlorine chemistry has never been probed on the Antarctic Plateau.

There is increasing body of evidence that heterogeneous hydrolysis of NO_2 can be a possible source of HONO and HNO_3 in acidic conditions (Finlayson-Pitts, 2009), with the potential to explain the difference between the calculated and measured atmospheric $\Delta^{17}O(NO_3^-)$ values. This mechanism would represent a source of nitrate with a $\Delta^{17}O$ value roughly equivalent to the nitrate originally present in the surface snow (i.e., 30–35 ‰), a signature significantly higher than that induced by R5. If this production mechanism is active at the air–snow interface at Dome C and results in the slow emission of nitrate to the atmosphere via physical release after its formation, it would act to increase the $\Delta^{17}O$ value of nitrate in the boundary layer relative to the local $\Delta^{17}O(NO_3^-)_{R5}$ oxidation signature. However, considering the propensity of nitric acid to stick on snow (Crowley et al., 2010), the snowpack to act as a sink rather than a source of nitric acid (Dibb, 2004; Erbland et al., 2013) and the fast NO_x recycling that should take place within the snowpack, it is very unlikely that $\Delta^{17}O(NO_3^-)$ could be explained by a direct nitric acid emissions from snow, which has been ultimately shown to be limited (Slusher et al., 2010; Erbland et al., 2013; Berhanu et al., 2014).

A critical analysis of $\Delta^{17}O(NO_3^-)$ shows in fact that such high values correspond mainly to the nighttime chemistry of NO_x (Michalski et al., 2003; Morin et al., 2008). Nighttime chemistry involves species like N_2O_5 and NO_3 in the process of forming HNO_3 and again efficiently bypass the OH pathway. It is conceivable that below the photic zone, within the snowpack, N_2O_5 and NO_3 could be produced when O_3 and NO_2 are transported at depth, but there is no reason to think that such dark NO_x chemistry could in one way or another survive the photic zone transition and thus influence the overlying atmosphere.

Stratospheric nitrate deposited to the surface snow during winter, which has been observed to possess $\Delta^{17}O(NO_3^-)$ values in the range of 35–41 ‰ (Erbland et al., 2013) and, possibly more, may act to buffer the $\Delta^{17}O$ of the atmospheric nitrate reservoir via evaporation late into the spring and summer. However, this seems again unlikely given the rapidity of NO_x cycling and oxidative loss at Dome C during this time (Frey et al., 2013; Legrand et al., 2009).

Alternatively, the discrepancy may originate from an systematic error in the $\Delta^{17}O$ values assigned to tropospheric ozone, specifically at Dome C (Fig. 3). In a 3-D global modeling exercise of $\Delta^{17}O(NO_3^-)$, Alexander et al. (2009) were able to reconcile modeling and observation only by assuming a bulk composition of ozone at $\Delta^{17}O = 35$ ‰ instead of the 25 ‰ generally assumed for the tropospheric ozone. While such high values would also solve our discrepancy, all observations and measurements published thus far are consistently closer to 25 ‰ than 35 ‰ (Vicars and Savarino, 2014; Johnston and Thiemens, 1997; Krankowsky et al., 1995). Given the low variability in the measurements observed at Dome C (Fig. 3) and elsewhere (Vicars and Savarino, 2014), if atmospheric measurements are underestimated, it should be by a systematic error common to both the liquid helium condensation or coated filter techniques. In the absence of such demonstration, we believe that the model–measurement discrepancy is likely due to false assumptions regarding NO_x chemistry or $^{17}O_{excess}$ transfer mechanisms. Equally, it is also possible that non-zero $\Delta^{17}O$ could be generated from know chemical reactions (i.e., well established) such as the CO + OH reaction which produces a positive $\Delta^{17}O$ in the remaining CO (Röckmann et al., 1998; Feilberg et al., 2005), although no evidence exists for this to occur. On the other hand, Table 2 shows that the variability in $\Delta^{17}O$ (but not the absolute values) is correctly caught by the model when α is constrained by the observations and $\Delta^{17}O(OH)$ by the observed HONO concentrations. This observation would favor the view that the chemistry and associated $\Delta^{17}O$ transfer are well understood and that a systematic error is likely at the origin of the discrepancy of the absolute values. However, this interpretation would be in contradiction with NO_x–HO_x chemistry observations showing that in fact such chemistry is not very well understood above the Antarctic ice sheet (Frey et al., 2015; Legrand et al., 2014; Slusher et al., 2010).

While it is presently difficult to determine the precise nature of the process(es) leading to the relatively large ^{17}O-excess values observed for atmospheric nitrate at Dome C, the correlation observed between the δ^{15}N and Δ^{17}O values of atmospheric nitrate (see Sect. 3.1) provides at least one direct line of evidence that the high $\Delta^{17}O(NO_3^-)$ values observed during spring and early summer could be associated with snowpack emissions of NO_x. Considering only samples collected at Dome C between October and December, both those reported here and those collected in 2009 and described by Erbland et al. (2013), a strong anticorrelation ($r = -0.90$) is observed between the δ^{15}N and Δ^{17}O values of atmospheric nitrate (Fig. 8). In other words, the atmospheric nitrate sampled in early spring, which is heavily depleted in ^{15}N due its formation from NO_x emissions arising from a winter-nitrified snowpack, possessed consistently higher Δ^{17}O values than the nitrate sampled directly after this period. Conversely, in summer, atmospheric nitrate possesses a lower Δ^{17}O and is ^{15}N enriched with respect to early spring values as it is formed from a snowpack that has suffered several stages of denitrification, leading to ^{15}N enrichment of the snowpack and the emitted NO_x. This finding suggests that the mechanism producing enhanced $\Delta^{17}O(NO_3^-)$ values observed during early spring is tightly coupled in time and space with the intensity of NO_x emissions from the snowpack, an observation very similar to that of Morin et al. (2012), who detected a similar relationship between δ^{15}N and Δ^{17}O for atmospheric nitrate in the springtime boundary layer over Barrow, Alaska (71° N). The authors of that study attributed the observed correlation to the coupling of snowpack NO_x emissions and reactive halogen chemistry, suggesting that these two processes were interrelated and mutually strengthening. In the case of the OPALE 2011–2012 data, the correlation between δ^{15}N and Δ^{17}O could arise from any of the potential pathways previously discussed. For example, as proposed by Morin et al. (2012), the R8 and R9 pathways may be enhanced during the period of polar sunrise. Alternatively, a correlation could result from an increased contribution to total OH production from the photolysis of HONO, which is co-emitted with NO_x via nitrate photochemistry (Grannas et al., 2007) and may induce a larger ^{17}O excess in OH as compared to the conventional $O(^1D) + H_2O$ pathway. Furthermore, the hydrolysis of NO_2 in snow, should it contribute significantly to nitrate production at Dome C, is likely amplified during periods when concentrations NO_2 are high in the snowpack interstitial air due to nitrate/nitrite photochemistry. Therefore, while the processes responsible for driving the formation of atmospheric nitrate at Dome C during summer cannot be unambiguously identified, the isotopic results presented here clearly indicate that snowpack emissions result in enhanced Δ^{17}O transfer to nitrate. Our understanding of NO_x chemistry above the snow surface at Dome C is therefore incomplete.

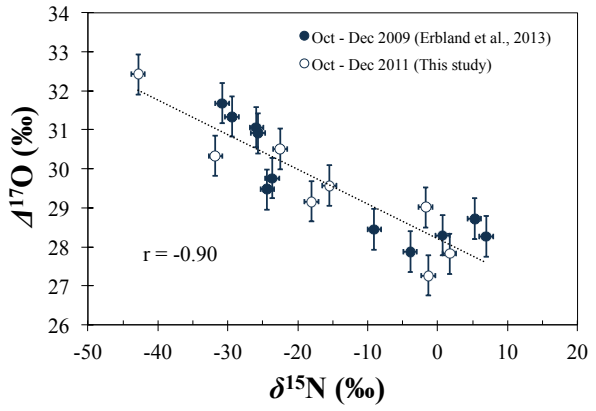

Figure 8. Relationship observed between the δ^{15}N and Δ^{17}O values of atmospheric nitrate present at Dome C between October and December during both the 2009 and 2011 summer campaigns. Error bars indicate the typical analytical uncertainties associated with the measurements.

5 Conclusions

Constraining the propagation of ozone's ^{17}O-excess signature within the NO_x cycle is critical in polar areas where the opportunity is offered to extend atmospheric investigations based on Δ^{17}O measurements to the glacial–interglacial timescale using deep ice core records of nitrate. However, the factors governing the present-day isotopic composition of atmospheric nitrate over the Antarctic Plateau remain poorly understood, primarily due to the complex nature of the boundary layer photochemistry initiated during spring by NO_x emissions from the snowpack.

An isotopic mass balance performed for atmospheric nitrate during December 2011, informed by in situ oxidant concentration measurements conducted within the framework of the OPALE field study, suggests the existence of an unexpected process bypassing the commonly accepted daytime chemistry of NO_2 (i.e., $NO_2 + OH$) that contributes significantly to the atmospheric nitrate budget over Dome C. The strong negative correlation observed between the δ^{15}N and Δ^{17}O values of nitrate between October and December suggests that this unknown process scales with the intensity of the snowpack photochemistry. Potential explanations for this observation include (i) an increased Δ^{17}O transfer from OH due to its formation from the photolysis of HONO released from the snowpack, (ii) heterogeneous hydrolysis of NO_2 due to the high concentrations of NO_2 in the snowpack interstitial air, and (iii) the co-emission of reactive halogen species that act as an intermediate in the transfer of Δ^{17}O from ozone to nitrate. Systematic measurement error and/or false assumptions regarding Δ^{17}O isotopic transfer functions cannot be completely excluded as potential causes for the observed discrepancy between the observed and modeled data. We encourage additional laboratory experiments to further reduce these uncertainties. However, given the other

lines of evidence presented here, we hypothesize that this discrepancy is due to an unknown or misunderstood component of the NO_x photochemical cycle over the Antarctic Plateau. Further research is needed to solve the many inconsistencies (e.g., high NO_2 / NO ratio, high concentration of NO_2, unresolved HONO atmospheric concentration, interference such as HO_2NO_2, isotope mass balance) observed during the OPALE experiments.

The Supplement related to this article is available online at doi:10.5194/acp-16-2659-2016-supplement.

Acknowledgements. The research leading to these results received funding from the European Community's Seventh Framework Programme (FP7/2007-2013) under the grant agreement number 237890. We would like to thank INSU for its financial support for lab experiments through its LEFE program. The Agence nationale de la recherche (ANR) is gratefully acknowledged for its financial support through the OPALE project (contract NT09-451281). The Institute Polaire Paul-Emile Victor (IPEV) supported the research and polar logistics through the program SUNITEDC No. 1011. This work has been partially supported by a grant from Labex OSUG@2020 (Investissements d'avenir – ANR10 LABX56). We would also like to thank all the field team members present during the OPALE campaign. Meteorological data were obtained from "IPEV/PNRA: Routine Meteorological Observation at Station Concordia". B. Alexander and the anonymous reviewer are acknowledged for their critical comments and suggestions, which helped in improving the manuscript. Data are available in the Supplement.

Edited by: T. Röckmann

References

Adon, M., Galy-Lacaux, C., Yoboué, V., Delon, C., Lacaux, J. P., Castera, P., Gardrat, E., Pienaar, J., Al Ourabi, H., Laouali, D., Diop, B., Sigha-Nkamdjou, L., Akpo, A., Tathy, J. P., Lavenu, F., and Mougin, E.: Long term measurements of sulfur dioxide, nitrogen dioxide, ammonia, nitric acid and ozone in Africa using passive samplers, Atmos. Chem. Phys., 10, 7467-7487, doi:10.5194/acp-10-7467-2010, 2010.

Alexander, B., Savarino, J., Kreutz, K., and Thiemens, M. H.: Impact of preindustrial biomass-burning emissions on the oxidative pathways of tropospheric sulfur and nitrogen, J. Geophys. Res., 109, D08303, doi:10.1029/2003JD004218, 2004.

Alexander, B., Hastings, M. G., Allman, D. J., Dachs, J., Thornton, J. A., and Kunasek, S. A.: Quantifying atmospheric nitrate formation pathways based on a global model of the oxygen isotopic composition ($\Delta^{17}O$) of atmospheric nitrate, Atmos. Chem. Phys., 9, 5043–5056, doi:10.5194/acp-9-5043-2009, 2009.

Anastasio, C. and Chu, L.: Photochemistry of Nitrous Acid (HONO) and Nitrous Acidium Ion (H_2ONO^+) in Aqueous Solution and Ice, Environ. Sci. Technol., 43, 1108–1114, doi:10.1021/es802579a, 2009.

Atkinson, R., Baulch, D. L., Cox, R. A., Crowley, J. N., Hampson, R. F., Hynes, R. G., Jenkin, M. E., Rossi, M. J., and Troe, J.: Evaluated kinetic and photochemical data for atmospheric chemistry: Volume I – gas phase reactions of O_x, HO_x, NO_x and SO_x species, Atmos. Chem. Phys., 4, 1461–1738, doi:10.5194/acp-4-1461-2004, 2004.

Atkinson, R., Baulch, D. L., Cox, R. A., Crowley, J. N., Hampson, R. F., Hynes, R. G., Jenkin, M. E., Rossi, M. J., and Troe, J.: Evaluated kinetic and photochemical data for atmospheric chemistry: Volume III – gas phase reactions of inorganic halogens, Atmos. Chem. Phys., 7, 981-1191, doi:10.5194/acp-7-981-2007, 2007.

Bauguitte, S. J.-B., Bloss, W. J., Evans, M. J., Salmon, R. A., Anderson, P. S., Jones, A. E., Lee, J. D., Saiz-Lopez, A., Roscoe, H. K., Wolff, E. W., and Plane, J. M. C.: Summertime NO_x measurements during the CHABLIS campaign: can source and sink estimates unravel observed diurnal cycles?, Atmos. Chem. Phys., 12, 989–1002, doi:10.5194/acp-12-989-2012, 2012.

Berhanu, T. A., Meusinger, C., Erbland, J., Jost, R., Bhattacharya, S. K., Johnson, M. S., and Savarino, J.: Laboratory study of nitrate photolysis in Antarctic snow. II. Isotopic effects and wavelength dependence, J. Chem. Phys., 140, 244305, doi:10.1063/1.4882899, 2014.

Bhattacharya, S. K., Pandey, A., and Savarino, J.: Determination of intramolecular isotope distribution of ozone by oxidation reaction with silver metal, J. Geophys. Res., 113, D03303, doi:10.1029/2006jd008309, 2008.

Bloss, W. J., Camredon, M., Lee, J. D., Heard, D. E., Plane, J. M. C., Saiz-Lopez, A., Bauguitte, S. J.-B., Salmon, R. A., and Jones, A. E.: Coupling of HO_x, NO_x and halogen chemistry in the antarctic boundary layer, Atmos. Chem. Phys., 10, 10187–10209, doi:10.5194/acp-10-10187-2010, 2010.

Bolton, D.: The Computation of Equivalent Potential Temperature, Mon. Weather Rev., 108, 1046–1053, 1980.

Casciotti, K. L., Sigman, D. M., Galanter Hastings, M., Böhlke, J. K., and Hilkert, A.: Measurement of the Oxygen Isotopic Composition of Nitrate in Seawater and Freshwater Using the Denitrifier Method, Anal. Chem., 74, 4905–4912, 2002.

Chen, G., Davis, D., Crawford, J., Nowak, J. B., Eisele, F., Mauldin, R. L., Tanner, D., Buhr, M., Shetter, R., Lefer, B., Arimoto, R., Hogan, A., and Blake, D.: An investigation of South Pole HO_x chemistry: Comparison of model results with ISCAT observations, Geophys. Res. Lett., 28, 3633–3636, doi:10.1029/2001GL013158, 2001.

Chen, G., Davis, D., Crawford, J., Hutterli, L. M., Huey, L. G., Slusher, D., Mauldin, L., Eisele, F., Tanner, D., Dibb, J., Buhr, M., McConnell, J., Lefer, B., Shetter, R., Blake, D., Song, C. H., Lombardi, K., and Arnoldy, J.: A reassessment of HO_x South Pole chemistry based on observations recorded during ISCAT 2000, Atmos. Environ., 38, 5451–5461, doi:10.1016/j.atmosenv.2003.07.018, 2004.

Coplen, T. B.: Guidelines and recommended terms for expression of stable-isotope-ratio and gas-ratio measurement results, Rapid Commun. Mass Sp., 25, 2538–2560, doi:10.1002/rcm.5129, 2011.

Crawford, J. H., Davis, D. D., Chen, G., Buhr, M., Oltmans, S., Weller, R., Mauldin, L., Eisele, F., Shetter, R., Lefer, B., Arimoto, R., and Hogan, A.: Evidence for photochemical production of

ozone at the South Pole surface, Geophys. Res. Lett., 28, 3641–3644, doi:10.1029/2001GL013055, 2001.

Crowley, J. N., Ammann, M., Cox, R. A., Hynes, R. G., Jenkin, M. E., Mellouki, A., Rossi, M. J., Troe, J., and Wallington, T. J.: Evaluated kinetic and photochemical data for atmospheric chemistry: Volume V – heterogeneous reactions on solid substrates, Atmos. Chem. Phys., 10, 9059–9223, doi:10.5194/acp-10-9059-2010, 2010.

Davis, D., Nowak, J. B., Chen, G., Buhr, M., Arimoto, R., Hogan, A., Eisele, F., Mauldin, L., Tanner, D., Shetter, R., Lefer, B., and McMurry, P.: Unexpected high levels of NO observed at South Pole, Geophys. Res. Lett., 28, 3625–3628, doi:10.1029/2000GL012584, 2001.

Davis, D., Seelig, J., Huey, G., Crawford, J., Chen, G., Wang, Y., Buhr, M., Helmig, D., Neff, W., and Blake, D.: A reassessment of Antarctic plateau reactive nitrogen based on ANTCI 2003 airborne and ground based measurements, Atmos. Environ., 42, 2831–2848, doi:10.1016/j.atmosenv.2007.07.039, 2008.

Dibb, J.: Soluble reactive nitrogen oxides at South Pole during ISCAT 2000, Atmos. Environ., 38, 5399–5409, doi:10.1016/j.atmosenv.2003.01.001, 2004.

Dubey, M. K., Mohrschladt, R., Donahue, N. M., and Anderson, J. G.: Isotope specific kinetics of hydroxyl radical (OH) with water (H_2O): Testing models of reactivity and atmospheric fractionation, J. Phys. Chem., 101, 1494–1500, 1997.

EPICA community members: Eight glacial cycles from an Antarctic ice core, Nature, 429, 623–628, doi:10.1038/nature02599, 2004.

Erbland, J., Vicars, W. C., Savarino, J., Morin, S., Frey, M. M., Frosini, D., Vince, E., and Martins, J. M. F.: Air–snow transfer of nitrate on the East Antarctic Plateau – Part 1: Isotopic evidence for a photolytically driven dynamic equilibrium in summer, Atmos. Chem. Phys., 13, 6403–6419, doi:10.5194/acp-13-6403-2013, 2013.

Fan, S.-M. and Jacob, D. J.: Surface ozone depletion in Arctic spring sustained by bromine reactions on aerosols, Nature, 359, 522–524, 1992.

Feilberg, K. L., Johnson, M. S., and Nielsen, C. J.: Relative rates of reaction of 13C16O, 12C18O, 12C17O and 13C18O with OH and OD radicals, Phys. Chem. Chem. Phys., 7, 2318, doi:10.1039/b503350k, 2005.

Finlayson-Pitts, B. J.: Reactions at surfaces in the atmosphere: integration of experiments and theory as necessary (but not necessarily sufficient) for predicting the physical chemistry of aerosols, Phys. Chem. Chem. Phys., 11, 7760–7779, doi:10.1039/b906540g, 2009.

France, J. L., King, M. D., Frey, M. M., Erbland, J., Picard, G., Preunkert, S., MacArthur, A., and Savarino, J.: Snow optical properties at Dome C (Concordia), Antarctica; implications for snow emissions and snow chemistry of reactive nitrogen, Atmos. Chem. Phys., 11, 9787–9801, doi:10.5194/acp-11-9787-2011, 2011.

Frey, M. M., Savarino, J., Morin, S., Erbland, J., and Martins, J. M. F.: Photolysis imprint in the nitrate stable isotope signal in snow and atmosphere of East Antarctica and implications for reactive nitrogen cycling, Atmos. Chem. Phys., 9, 8681–8696, doi:10.5194/acp-9-8681-2009, 2009.

Frey, M. M., Brough, N., France, J. L., Anderson, P. S., Traulle, O., King, M. D., Jones, A. E., Wolff, E. W., and Savarino, J.: The diurnal variability of atmospheric nitrogen oxides (NO and NO_2) above the Antarctic Plateau driven by atmospheric stability and snow emissions, Atmos. Chem. Phys., 13, 3045–3062, doi:10.5194/acp-13-3045-2013, 2013.

Frey, M. M., Roscoe, H. K., Kukui, A., Savarino, J., France, J. L., King, M. D., Legrand, M., and Preunkert, S.: Atmospheric nitrogen oxides (NO and NO_2) at Dome C, East Antarctica, during the OPALE campaign, Atmos. Chem. Phys., 15, 7859–7875, doi:10.5194/acp-15-7859-2015, 2015.

Gane, M. P., Williams, N. A., and Sodeau, J. R.: A reflection-absorption infrared spectroscopy (RAIRS) investigation of the low-temperature heterogeneous hydrolysis of bromine nitrate, J. Phys. Chem. A, 105, 4002–4009, 2001.

Geyh, A., Wolfson, J. M., and Koutrakis, P.: Development and Evaluation of a Small Active Ozone Sampler, Environ. Sci. Technol., 31, 2326–2330, 1997.

Granger, J. and Sigman, D. M.: Removal of nitrite with sulfamic acid for nitrate N and O isotope analysis with the denitrifier method, Rapid Commun. Mass Sp., 23, 3753–3762, doi:10.1002/rcm.4307, 2009.

Grannas, A. M., Jones, A. E., Dibb, J., Ammann, M., Anastasio, C., Beine, H. J., Bergin, M., Bottenheim, J., Boxe, C. S., Carver, G., Chen, G., Crawford, J. H., Dominé, F., Frey, M. M., Guzmán, M. I., Heard, D. E., Helmig, D., Hoffmann, M. R., Honrath, R. E., Huey, L. G., Hutterli, M., Jacobi, H. W., Klán, P., Lefer, B., McConnell, J., Plane, J., Sander, R., Savarino, J., Shepson, P. B., Simpson, W. R., Sodeau, J. R., von Glasow, R., Weller, R., Wolff, E. W., and Zhu, T.: An overview of snow photochemistry: evidence, mechanisms and impacts, Atmos. Chem. Phys., 7, 4329–4373, doi:10.5194/acp-7-4329-2007, 2007.

Hastings, M. G., Sigman, D. M., and Steig, E. J.: Glacial/interglacial changes in the isotopes of nitrate from the Greenland Ice Sheet Project 2 (GISP2) ice core, Global Biogeochem. Cy., 19, GB4024, doi:10.1029/2005gb002502, 2005.

Hastings, M. G., Jarvis, J. C., and Steig, E. J.: Anthropogenic impacts on nitrogen isotopes of ice-core nitrate, Science, 324, 1288–1288, doi:10.1126/science.1170510, 2009.

Honrath, R. E., Peterson, M. C., Guo, S., Dibb, J. E., Shepson, P. B., and Campbell, B.: Evidence of NO_x production within or upon ice particles in the Greenland snowpack, Geophys. Res. Lett., 26, 695–698, 1999.

Honrath, R. E., Guo, S., Peterson, M. C., Dziobak, M. P., Dibb, J. E., and Arsenault, M. A.: Photochemical production of gas phase NO_x from ice crystal NO_3, J. Geophys. Res., 105, 24183–24190, 2000.

Hutterli, M. A., McConnell, J. R., Bales, R. C., and Stewart, R. W.: Sensitivity of hydrogen peroxide (H_2O_2) and formaldehyde (HCHO) preservation in snow to changing environmental conditions: Implications for ice core records, J. Geophys. Res.-Atmos., 108, 4023, doi:10.1029/2002JD002528, 2003.

Jacobi, H. W. and Hilker, B.: A mechanism for the photochemical transformation of nitrate in snow, J. Photoch. Photobiol. A, 185, 371–382, doi:10.1016/j.jphotochem.2006.06.039, 2007.

Janssen, C. and Tuzson, B.: A diode laser spectrometer for symmetry selective detection of ozone isotopomers, Appl. Phys. B, 82, 487–494, doi:10.1007/s00340-005-2044-6, 2006.

Jarvis, J. C., Steig, E. J., Hastings, M. G., and Kunasek, S. A.: Influence of local photochemistry on isotopes of nitrate in Greenland snow, Geophys. Res. Lett., 35, L21804, doi:10.1029/2008gl035551, 2008.

Johnston, J. C. and Thiemens, M. H.: The isotopic composition of tropospheric ozone in three environments, J. Geophys. Res., 102, 25395–25404, 1997.

Jones, A. E., Weller, R., Wolff, E. W., and Jacobi, H.-W.: Speciation and rate of photochemical NO and NO_2 production in Antarctica snow, Geophys. Res. Lett., 27, 345–348, 2000.

Jones, A. E., Weller, R., Anderson, P. S., Jacobi, H. W., Wolff, E. W., Schrems, O., and Miller, H.: Measurements of NO_x emissions from the Antarctic snowpack, Geophys. Res. Lett., 28, 1499–1502, 2001.

Jourdain, B., Preunkert, S., Cerri, O., Castebrunet, H., Udisti, R., and Legrand, M.: Year-round record of size-segregated aerosol composition in central Antarctica (Concordia station): Implications for the degree of fractionation of sea-salt particles, J. Geophys. Res., 113, D14308, doi:10.1029/2007jd009584, 2008.

Kaiser, J., Hastings, M. G., Houlton, B. Z., Röckmann, T., and Sigman, D. M.: Triple oxygen isotope analysis of nitrate using the denitrifier method and thermal decomposition of N_2O, Anal. Chem., 79, 599–607, 2007.

Koutrakis, P., Wolfson, J. M., Bunyaviroch, A., Froehlich, S. E., Hirano, K., and Muliki, J. D.: Measurement of Ambient Ozone Using a Nitrite-Coated Filter, Anal Chem, 65, 209–214, 1993.

Krankowsky, D., Bartecki, F., Klees, G. G., Mauersberger, K., Schellenbach, K., and Stehr, J.: Measurement of heavy isotope enrichment in tropospheric ozone, Geophys. Res. Lett., 22, 1713–1716, 1995.

Krzyzanowski, J.: Ozone variation with height in a forest canopy – results from a passive sampling field campaign, Atmos. Environ., 38, 5957–5962, doi:10.1016/j.atmosenv.2004.07.017, 2004.

Kukui, A., Legrand, M., Preunkert, S., Frey, M. M., Loisil, R., Gil Roca, J., Jourdain, B., King, M. D., France, J. L., and Ancellet, G.: Measurements of OH and RO_2 radicals at Dome C, East Antarctica, Atmos. Chem. Phys., 14, 12373–12392, doi:10.5194/acp-14-12373-2014, 2014.

Legrand, M., Preunkert, S., Jourdain, B., Gallée, H., Goutail, F., Weller, R., and Savarino, J.: Year-round record of surface ozone at coastal (Dumont d'Urville) and inland (Concordia) sites in East Antarctica, J. Geophys. Res., 114, D20306, doi:10.1029/2008jd011667, 2009.

Legrand, M., Preunkert, S., Frey, M., Bartels-Rausch, Th., Kukui, A., King, M. D., Savarino, J., Kerbrat, M., and Jourdain, B.: Large mixing ratios of atmospheric nitrous acid (HONO) at Concordia (East Antarctic Plateau) in summer: a strong source from surface snow?, Atmos. Chem. Phys., 14, 9963–9976, doi:10.5194/acp-14-9963-2014, 2014.

Legrand, M., Preunkert, S., Savarino, J., Frey, M. M., Kukui, A., Helmig, D., Jourdain, B., Jones, A., Weller, R., Brough, N., and Gallée, H.: Inter-annual variability of surface ozone at coastal (Dumont d'Urville, 2004–2014) and inland (Concordia, 2007–2014) sites in East Antarctica, Atmos. Chem. Phys. Discuss., doi:10.5194/acp-2016-95, in review, 2016.

Liao, W. and Tan, D.: 1-D Air-snowpack modeling of atmospheric nitrous acid at South Pole during ANTCI 2003, Atmos. Chem. Phys., 8, 7087–7099, doi:10.5194/acp-8-7087-2008, 2008.

Luz, B. and Barkan, E.: Variations of $^{17}O/^{16}O$ and $^{18}O/^{16}O$ in meteoric waters, Geochim. Cosmochim. Ac., 74, 6276–6286, doi:10.1016/j.gca.2010.08.016, 2010.

Mauldin, R. L., Eisele, F. L., Tanner, D. J., Kosciuch, E., Shetter, R., Lefer, B., Hall, S. R., Nowak, J. B., Buhr, M., Chen, G., Wang, P., and Davis, D.: Measurements of OH, H_2SO_4, and MSA at the South Pole during ISCAT, Geophys. Res. Lett., 28, 3629–3632, 2001.

McCabe, J. R., Boxe, C. S., Colussi, A. J., Hoffman, M. R., and Thiemens, M. H.: Oxygen isotopic fractionation in the photochemistry of nitrate in water and ice, J. Geophys. Res., 110, D15310, 10.1029/2004jd005484, 2005.

McCabe, J. R., Thiemens, M. H., and Savarino, J.: A record of ozone variability in South Pole Antarctic snow: Role of nitrate oxygen isotopes, J. Geophys. Res., 112, D12303, doi:10.1029/2006jd007822, 2007.

McNamara, J. P. and Hillier, I. H.: Mechanism of the hydrolysis of halogen nitrates in small water clusters studied by electronic structure methods, J. Phys. Chem. A, 105, 7011–7024, 2001.

Michalski, G., Savarino, J., Bohlke, J. K., and Thiemens, M.: Determination of the total oxygen isotopic composition of nitrate and the calibration of a Delta O-17 nitrate reference material, Anal. Chem., 74, 4989–4993, doi:10.1021/ac0256282, 2002.

Michalski, G., Scott, Z., Kabiling, M., and Thiemens, M. H.: First measurements and modeling of $\Delta^{17}O$ in atmospheric nitrate, Geophys. Res. Lett., 30, 1870, doi:10.1029/2003gl017015, 2003.

Michalski, G., Böhlke, J. K., and Thiemens, M.: Long term atmospheric deposition as the source of nitrate and other salts in the Atacama Desert, Chile: New evidence from mass-independent oxygen isotopic compositions, Geochim. Cosmochim. Ac., 68, 4023–4038, doi:10.1016/j.gca.2004.04.009, 2004.

Michalski, G., Bhattacharya, S. K., and Girsch, G.: NO_x cycle and the tropospheric ozone isotope anomaly: an experimental investigation, Atmos. Chem. Phys., 14, 4935–4953, doi:10.5194/acp-14-4935-2014, 2014.

Morin, S., Savarino, J., Bekki, S., Gong, S., and Bottenheim, J. W.: Signature of Arctic surface ozone depletion events in the isotope anomaly ($\Delta^{17}O$) of atmospheric nitrate, Atmos. Chem. Phys., 7, 1451–1469, doi:10.5194/acp-7-1451-2007, 2007.

Morin, S., Savarino, J., Yan, N., Frey, M. M., Bottenheim, J., Bekki, S., and Martins, J.: Tracing the origin and fate of NO_x in the Arctic atmosphere using stable isotopes, Science, 322, 730–732, doi:10.1126/science.1161910, 2008.

Morin, S., Savarino, J., Frey, M. M., Domine, F., Jacobi, H. W., Kaleschke, L., and Martins, J. M. F.: Comprehensive isotopic composition of atmospheric nitrate in the Atlantic Ocean boundary layer from 65° S to 79° N, J. Geophys. Res., 114, D05303, doi:10.1029/2008jd010696, 2009.

Morin, S., Sander, R., and Savarino, J.: Simulation of the diurnal variations of the oxygen isotope anomaly ($\Delta^{17}O$) of reactive atmospheric species, Atmos. Chem. Phys., 11, 3653–3671, doi:10.5194/acp-11-3653-2011, 2011.

Morin, S., Erbland, J., Savarino, J., Domine, F., Bock, J., Friess, U., Jacobi, H. W., Sihler, H., and Martins, J. M. F.: An isotopic view on the connection between photolytic emissions of NO_x from the Arctic snowpack and its oxidation by reactive halogens, J. Geophys. Res.-Atmos., 117, D00R08, doi:10.1029/2011jd016618, 2012.

Murray, L. T., Mickley, L. J., Kaplan, J. O., Sofen, E. D., Pfeiffer, M., and Alexander, B.: Factors controlling variability in the oxidative capacity of the troposphere since the Last Glacial Maximum, Atmos. Chem. Phys., 14, 3589–3622, doi:10.5194/acp-14-3589-2014, 2014.

Petit, J. R., Jouzel, J., Raynaud, D., Barkov, N. I., Barnola, J. M., Basile, I., Bender, M., Chappellaz, J., Davis, M., Delaygue, G., Delmotte, M., Kotlyakov, V. M., Legrand, M., Lipenkov, V. Y., Lorius, C., Pepin, L., Ritz, C., Saltzman, E., and Stievenard, M.: Climate and atmospheric history of the past 420,000 years from the Vostok ice core, Antarctica, Nature, 399, 429–436, 1999.

Preunkert, S., Jourdain, B., Legrand, M., Udisti, R., Becagli, S., and Cerri, O.: Seasonality of sulfur species (dimethyl sulfide, sulfate, and methanesulfonate) in Antarctica: Inland versus coastal regions, J. Geophys. Res., 113, D15302, doi:10.1029/2008jd009937, 2008.

Preunkert, S., Ancellet, G., Legrand, M., Kukui, A., Kerbrat, M., Sarda-Estève, R., Gros, V., and Jourdain, B.: Oxidant Production over Antarctic Land and its Export (OPALE) project: An overview of the 2010–2011 summer campaign, J. Geophys. Res.-Atmos., 117, D15307, doi:10.1029/2011JD017145, 2012.

Röckmann, T., Brenninkmeijer, C. A. M., Saueressig, G., Bergamaschi, P., Crowley, J. N., Fisher, H., and Crutzen, P. J.: Mass-independent oxygen isotope fractionation in atmospheric CO as a result of the reaction CO + OH, Science, 281, 544–546, 1998.

Röckmann, T., Kaiser, J., Brenninkmeijer, C. A. M., Crowley, J. N., Borchers, R., Brand, W. A., and Crutzen, P. J.: Isotopic enrichment of nitrous oxide ($^{15}N^{14}NO$), ($^{14}N^{15}NO$), ($^{14}N^{14}N^{18}O$) in the stratosphere and in the laboratory, J. Geophys. Res., 106, 10403–10410, 2001.

Sander, R., Rudich, Y., von Glasow, R., and Crutzen, P. J.: The role of $BrNO_3$ in marine tropospheric chemistry: A model study, Geophys. Res. Lett., 26, 2857–2860, 1999.

Savarino, J., Kaiser, J., Morin, S., Sigman, D. M., and Thiemens, M. H.: Nitrogen and oxygen isotopic constraints on the origin of atmospheric nitrate in coastal Antarctica, Atmos. Chem. Phys., 7, 1925–1945, doi:10.5194/acp-7-1925-2007, 2007.

Savarino, J., Bhattacharya, S. K., Morin, S., Baroni, M., and Doussin, J. F.: The $NO + O_3$ reaction: A triple oxygen isotope perspective on the reaction dynamics and atmospheric implications for the transfer of the ozone isotope anomaly, J. Chem. Phys., 128, 194303, doi:10.1063/1.2917581, 2008.

Savarino, J., Morin, S., Erbland, J., Grannec, F., Patey, M. D., Vicars, W., Alexander, B., and Achterberg, E. P.: Isotopic composition of atmospheric nitrate in a tropical marine boundary layer, P. Natl. Acad. Sci., 110, 17668–17673, doi:10.1073/pnas.1216639110, 2013.

Sigg, A. and Neftel, A.: Evidence For a 50-Percent Increase in H_2O_2 Over the Past 200 Years From a Greenland Ice Core, Nature, 351, 557–559, 1991.

Sigman, D. M., Casciotti, K. L., Andreani, M., Barford, C., Galanter, M., and Böhlke, J. K.: A bacterial method for the nitrogen isotopic analysis of nitrate in seawater and freshwater, Anal. Chem., 73, 4145–4153, 2001.

Simpson, W. R., von Glasow, R., Riedel, K., Anderson, P., Ariya, P., Bottenheim, J., Burrows, J., Carpenter, L. J., Frieß, U., Goodsite, M. E., Heard, D., Hutterli, M., Jacobi, H.-W., Kaleschke, L., Neff, B., Plane, J., Platt, U., Richter, A., Roscoe, H., Sander, R., Shepson, P., Sodeau, J., Steffen, A., Wagner, T., and Wolff, E.: Halogens and their role in polar boundary-layer ozone depletion, Atmos. Chem. Phys., 7, 4375–4418, doi:10.5194/acp-7-4375-2007, 2007.

Slusher, D. L., Neff, W. D., Kim, S., Huey, L. G., Wang, Y., Zeng, T., Tanner, D. J., Blake, D. R., Beyersdorf, A., Lefer, B. L., Crawford, J. H., Eisele, F. L., Mauldin, R. L., Kosciuch, E., Buhr, M. P., Wallace, H. W., and Davis, D. D.: Atmospheric chemistry results from the ANTCI 2005 Antarctic plateau airborne study, J. Geophys. Res., 115, D07304, doi:10.1029/2009jd012605, 2010.

Staffelbach, T., Neftel, A., Stauffer, B., and Jacob, D.: A record of the atmospheric methane sink from formaldehyde in polar ice cores, Nature, 349, 603–605, 1991.

Thiemens, M. H.: History and applications of mass-independent isotope effects, Annu. Rev. Earth Planet. Sc., 34, 217–262, 2006.

Thompson, A. M.: The oxidizing capacity of the Earth's atmosphere – Probable past and futur changes, Science, 256, 1157–1165, 1992.

Vicars, W. C. and Savarino, J.: Quantitative constraints on the ^{17}O-excess ($\Delta^{17}O$) signature of surface ozone: Ambient measurements from 50° N to 50° S using the nitrite-coated filter technique, Geochim. Cosmochim. Ac., 135, 270–287, doi:10.1016/j.gca.2014.03.023, 2014.

Vicars, W. C., Bhattacharya, S. K., Erbland, J., and Savarino, J.: Measurement of the ^{17}O-excess ($\Delta^{17}O$) of tropospheric ozone using a nitrite-coated filter, Rapid Commun. Mass Sp., 26, 1219–1231, doi:10.1002/rcm.6218, 2012.

Vicars, W. C., Morin, S., Savarino, J., Wagner, N. L., Erbland, J., Vince, E., Martins, J. M. F., Lerner, B. M., Quinn, P. K., Coffman, D. J., Williams, E. J., and Brown, S. S.: Spatial and diurnal variability in reactive nitrogen oxide chemistry as reflected in the isotopic composition of atmospheric nitrate: Results from the CalNex 2010 field study, J. Geophys. Res.-Atmos., 118, 10567–10588, doi:10.1002/jgrd.50680, 2013.

Vogt, R., Crutzen, P. J., and Sander, R.: A mechanism for halogen release from sea-salt aerosol in the remote marine boundary layer, Nature, 383, 327–330, 1996.

Wang, Y., Choi, Y., Zeng, T., Davis, D., Buhr, M., Gregoryhuey, L., and Neff, W.: Assessing the photochemical impact of snow NO_x emissions over Antarctica during ANTCI 2003, Atmos. Environ., 41, 3944–3958, doi:10.1016/j.atmosenv.2007.01.056, 2007.

Wang, Y. H. and Jacob, D. J.: Anthropogenic forcing on tropospheric ozone and OH since preindustrial times, J. Geophys. Res.-Atmos., 103, 31123–31135, 1998.

Werner, R. A. and Brand, W. A.: Referencing strategies and techniques in stable isotope ratio analysis, Rapid Commun. Mass Sp., 15, 501–519, doi:10.1002/rcm.258, 2001.

Zahn, A., Franz, P., Bechtel, C., Grooß, J.-U., and Röckmann, T.: Modelling the budget of middle atmospheric water vapour isotopes, Atmos. Chem. Phys., 6, 2073–2090, doi:10.5194/acp-6-2073-2006, 2006.

Zhang, J. S., Miau, T. T., and Lee, Y. T.: Crossed molecular beam study of the reaction $Br + O_3$, J. Phys. Chem. A, 101, 6922–6930, 1997.

Zhou, X., Beine, H. J., Honrath, R. E., Fuentes, J. D., Simpson, W., Shepson, P. B., and Bottenheim, J. W.: Snowpack photochemical production of HONO: A major source of OH in the Arctic boundary layer in springtime, Geophys. Res. Lett., 28, 4087–4090, doi:10.1029/2001GL013531, 2001.